JOURNAL OF Materials CHEMISTRY

Ionic liquid crystals: hexafluorophosphate salts

Charles M. Gordon,*[a] John D. Holbrey,[b] Alan R. Kennedy[a] and Kenneth R. Seddon[b]

[a]*Department of Pure and Applied Chemistry, University of Strathclyde, Thomas Graham Building, 295 Cathedral Street, Glasgow, UK G1 1XL. E-mail: c.m.gordon@strath.ac.uk*
[b]*The QUESTOR Centre, The Queen's University of Belfast, Stranmillis Road, Belfast, Northern Ireland, UK BT9 5AG*

Received 5th August 1998, Accepted 19th October 1998

A series of novel hexafluorophosphate salts, based on *N,N′*-dialkylimidazolium and substituted *N*-alkylpyridinium cations, display liquid crystalline behaviour at temperatures above their melting point. The temperature range over which liquid crystalline behaviour is observed increases markedly with increasing alkyl chain length. Alkyl substitution at the 3- and 4-positions on the pyridinium ring results in a decrease in the melting point compared with the equivalent unsubstituted salt, but also leads to a large decrease in the tendency towards liquid crystalline behaviour (or mesogenicity). The salts prepared are fully characterised using a wide variety of techniques, including NMR and IR spectroscopy, DSC, and single crystal X-ray diffraction in the case of 1-dodecyl-3-methylimidazolium hexafluorophosphate. The effect of preparing mixtures containing different proportions of two cations is also reported.

Introduction

A large variety of molecular thermotropic liquid crystalline materials have been prepared. In comparison, only a limited range of ionic liquid crystalline species is known. Alkali metal soaps were the first salts identified as displaying this type of behaviour,[1] followed more recently by amphiphilic alkylammonium[2] and *N*-alkylpyridinium salts.[3] Amphiphilic 1-methyl-4-alkylpyridinium iodides have also been shown to display thermotropic liquid crystalline behaviour.[4] Liquid crystalline *and* thermochromic behaviour has been observed in 1-methyl-4-*n*-alkoxycarbonylpyridinium[4] and 1-hexadecyl-4-cyanopyridinium iodide salts.[5] Further developments have involved the replacement of the 1-alkyl group with mesogens,[6,7] while recent publications have demonstrated thermotropic liquid crystalline behaviour in 1-alkyl-4-cholesterylpyridinium,[8] 1-ethyl-4-(5-alkyl-1,3-dioxan-2-yl)pyridinium,[9] and 1-alkylstilbazolium halide salts.[10] All of these studies have concentrated on halide salts; only a few papers report ionic liquid crystalline materials containing other anions, notably metallomesogens,[11] $[MCl_4]^{2-}$ (M = Co, Ni),[12] $[ZnBr_4]^{2-}$,[13] $[C_{12}H_{25}OSO_3]^-$,[14] and hydrogentartrate.[15] Practical applications of these materials are limited, particularly in the case of the simple alkylammonium salts, by the high melting points of the systems studied. A recent investigation of transition metal salts based on long chain 1-alkyl-3-methylimidazolium and *N*-alkylpyridinium cations showed that these possess relatively low melting points, combined with large mesophase ranges,[12] thus showing greater potential for further development.

Our interest in ionic liquid crystals arose from the study of low melting ionic liquids. Ionic liquids is now a commonly accepted term for low melting molten salts, and these materials are finding increasing application as solvents, particularly in the area of clean technology as controls on conventional solvents such as chlorinated hydrocarbons become more stringent.[16] Ionic liquids are prepared by combining bulky organic cations such as 1-butyl-3-methylimidazolium or 1-butylpyridinium with a wide variety of anions. The properties of ionic liquids can be controlled to a large degree by variation in the nature of both the cation and the anion. The effect of altering the anion has been quite widely investigated: for example, salts based on aluminium(III) chloride may be prepared which are Franklin acidic or basic, and extremely water sensitive, while those based on anions such as triflate and hexafluorophosphate are neutral and extremely hydrophobic.[17] By way of comparison, the effect of chemical modification of the cation has been little studied. An increasing chain length in the cation will be expected to result in an alteration in the melting point, and an increase in the viscosity and hydrophobicity of the liquids. A further effect, once chain lengths of a sufficient length are present, will be the formation of liquid crystalline phases on melting, as shown by the examples described in the previous paragraph.

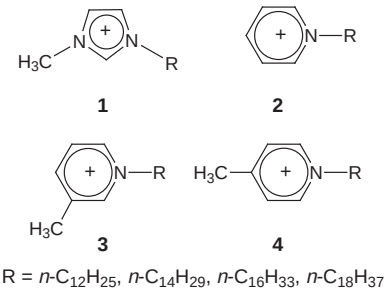

Fig. 1 Structures of the organic cations employed.

One ionic liquid which is finding increasing use is 1-butyl-3-methylimidazolium hexafluorophosphate, [bmim][PF_6], an easily prepared, almost completely water insoluble liquid, which has been used as a solvent for two-phase catalysis reactions.[18] In this study, we report the liquid crystalline properties of some hexafluorophosphate salts of alkyl-substituted imidazolium ([R-mim]$^+$ **1**), pyridinium ([R-py]$^+$ **2**), 3- and 4-methylpyridinium ([R-3-Mepy]$^+$ **3** and [R-4-Mepy]$^+$ **4**) cations,† as indicated in Fig. 1.

Such salts are potentially of great interest as ordered ionic solvents, combining the advantages of ionic liquids with those of liquid crystal solvents. The aim of this study was to identify systems that combined a relatively low melting point with a large mesophase range. Once the principles influencing the thermal behaviour of these salts are understood, the intention is to develop more sophisticated systems that can be employed as ordered solvents. The application of more 'traditional'

†Henceforth all cations will be referred to using the shortened form of the cation name, and the alkyl chain simply by its number of carbon atoms, *i.e.* [C_{12}-mim] = 1-*n*-dodecyl-3-methylimidazolium.

molecular liquid crystalline materials as ordered solvents for polymerisation[19] and stereochemically controlled organic reactions[20] is an area of increasing interest. Only one other related liquid crystalline salt containing the hexafluorophosphate anion has been reported: the symmetrically substituted 1,3-dihexadecylimidazolium hexafluorophosphate, for which transition temperatures and energies were recently reported.[21]

Experimental

Aqueous hexafluorophosphoric acid (60% w/w, *ex*-Aldrich), pyridine, 3-methylpyridine and 4-methylpyridine (*ex*-Aldrich) were used as received. 1-Methylimidazole (*ex*-Aldrich) was purified by distillation from KOH. 1-Chlorododecane, 1-chlorotetradecane, 1-chlorohexadecane and 1-chlorooctadecane (*ex*-Lancaster or Aldrich) were used as received. Acetone-d_6 was purchased from Goss Scientific Instruments Ltd. Acetonitrile was dried by distillation from CaH_2.

Synthesis of salts

Chloride salts were prepared by mixing equimolar quantities of the appropriate amine and chloroalkane in a Carius tube in a dinitrogen-filled drybox. The tube was removed from the drybox, degassed at $-196\,^{\circ}C$, sealed under vacuum, and heated at 100 °C for 7 days, or until reaction was observed to be complete (the mixture formed a single viscous phase). The tube was then cooled, and opened in the drybox. The crude solid product was removed, recrystallised from dry CH_3CN, and then stored in the drybox until use. In general, the halide salts became less hygroscopic as the alkyl chain increased in length. The amines employed were 1-methylimidazole, pyridine, and 3- and 4-methylpyridine; salts were prepared with alkyl chain lengths C_{12}, C_{14}, C_{16} and C_{18}.

The hexafluorophosphate salts were prepared by reaction of the appropriate chloride salt with HPF_6 in aqueous solution. As the method was effectively identical for all salts, the exact method employed for [C_{14}-py][PF_6] will be discussed as a representative example: [C_{14}-py]Cl (1.00 g, 3.20 mmol) was dissolved in water (20 cm^3), and then cooled to 0 °C in an ice bath. The mixture was stirred vigorously and 60% w/w HPF_6 solution (1.0 cm^3, 6.80 mmol) was added using a glass syringe. A rapid exothermic reaction then occurred, with the product forming as an insoluble white solid. This was collected by filtration, washed with a large excess of water to remove any remaining traces of HPF_6, then recrystallised from a minimum quantity of methanol, and dried *in vacuo*. A final yield of 0.73 g (54.0%) was obtained. The solubility in methanol increased with decreasing chain length, generally resulting in somewhat lower yields for the shortest chain length products and higher yields for the salts with longer alkyl chains. The pure recrystallised product formed as white plates, which were dried in a vacuum desiccator for at least 24 h. The purity of all the salts was checked by ^1H NMR spectroscopy (in acetone-d_6), microanalysis (see Table 1) and DSC (see later).

Mixtures of two salts were prepared by carefully weighing out the appropriate molar ratios of [C_{16}-mim][PF_6] and [C_{16}-py][PF_6]. The mixtures were then ground thoroughly, heated to a temperature well above their clearing points, and then allowed to cool. This process was repeated three times for the resulting solids, by which stage it was assessed that broadly homogeneous mixtures had been prepared.

Analytical methods

^1H NMR spectra were recorded in acetone-d_6 solution on 400 MHz Bruker AMX400 or 250 MHz Bruker WM250 FT NMR spectrometers. IR spectra were run as KBr disks on a Nicolet Impact 400D FTIR spectrometer. FAB mass spectrometry was performed on a JEOL JMS-AX505HA instrument, using a glycerol matrix.

Thermal investigations

DSC measurements were carried out using a Perkin Elmer DSC 2 or Perkin Elmer DSC 7. Heating and cooling rates of $10\,^{\circ}C\,min^{-1}$ were typically employed. Each sample was preheated to its clearing point, allowed to cool to its crystallisation point, and then reheated for data collection. Polarised optical microscopy (POM) studies on the salts were carried out using an Olympus Vanox microscope under cross-polarised light at $100\times$ magnification. The samples were placed between two cover slips and heated using a Linkam PR600 hot stage, which permitted control of the temperature to $\pm 0.1\,^{\circ}C$. Heating and cooling rates of $10\,^{\circ}C\,min^{-1}$ were once again generally employed, except when a very precise determination of transition temperatures was required, in which case slower rates were used. As with the DSC measurements, data were only recorded after the sample had first been heated to its clearing point and then allowed to cool to its crystallisation point. Photographs of the mesophase were taken at the same magnification using a Polaroid Micro SLR camera.

Experimental crystallography

(i) Powder X-ray diffraction. Powder X-ray diffraction studies were made at room temperature with Cu-Kα X-rays, ($\lambda = 1.542$ Å) using a Siemens D5000 powder diffractometer. Data were recorded in the range 2–20° in steps of 0.05°.

(ii) Single crystal X-ray diffraction. Crystals of [C_{12}-mim][PF_6] were grown by slow evaporation of a methanolic solution of the salt. Crystal data, data collection and refinement parameters are given in Table 2. Measurements were made at 123 K with Mo-Kα X-rays, ($\lambda = 0.71069$ Å), on a Rigaku AFC7S diffractometer fitted with a graphite monochromator. Cell dimensions were based on 25 reflections with $18.2 < 2\theta < 34.8°$. Intensities, I, were derived from ω–2θ scans, and corrections were applied for Lorentz polarisation and absorption effects, the latter based on averaging several azimuthal scans. Equivalent intensities were then averaged and unobserved reflections with $I < 2\sigma(I)$ excluded from further consideration.

The structure was solved by direct methods[22] and the examination of subsequent difference syntheses. All non-hydrogen atoms were refined anisotropically. H atoms were positioned as found with $B_{iso} = 1.2B_{eq}$ of the parent atom. An isotropic extinction parameter [$5.4(8) \times 10^{-7}$] was also refined. Final full-matrix, least-squares refinement was on F with $w = 1/\sigma^2(F)$ and converged to give a maximum shift/esd ratio of 0.003. All calculations were performed on a Silicon Graphics Indy R4600 with the teXsan set of programs.[23]

Full crystallographic details, excluding structure factors, have been deposited at the Cambridge Crystallographic Data Centre (CCDC). See Information for Authors, *J. Mater. Chem.*, 1998, Issue 1. Any request to the CCDC for this material should quote the full literature citation and the reference number 1145/1046.

See http://www.rsc.org/suppdata/jm/1998/2627/for crystallographic details in cif format.

Results

As stated above, *N*-alkyl substituted 1-methylimidazolium, pyridinium, 3- and 4-methylpyridinium hexafluorophosphate salts were prepared with alkyl chain lengths of C_{12}, C_{14}, C_{16}, and C_{18}. Halide and tetrachlorometallate salts of some of these cations have been shown previously to display liquid crystalline phases at temperatures above their melting points.[3,12] The products were prepared in aqueous solution by metathesis of the appropriate organic cation halide with HPF_6. The white crystalline solid products were insoluble in water, and were thus simply collected by filtration. Purification was

Table 1 Microanalytical data for anhydrous [Q][PF_6] salts

Q^+	C % found (calc.)	H % found (calc.)	N % found (calc.)
C_{12}-mim	48.6 (48.4)	8.2 (7.9)	7.0 (7.1)
C_{14}-mim	51.0 (50.9)	8.6 (8.3)	6.6 (6.6)
C_{16}-mim	53.1 (53.1)	8.9 (8.7)	6.1 (6.2)
C_{18}-mim	54.9 (55.0)	9.1 (9.0)	5.7 (5.8)
C_{12}-py	52.0 (51.9)	7.9 (7.7)	3.5 (3.6)
C_{14}-py	54.3 (54.1)	8.5 (8.1)	3.3 (3.3)
C_{16}-py	55.7 (56.1)	8.5 (8.5)	3.0 (3.1)
C_{18}-py	57.6 (57.8)	9.0 (8.9)	3.0 (2.9)
C_{12}-3-Mepy	53.0 (53.1)	8.2 (7.9)	3.4 (3.4)
C_{14}-3-Mepy	55.2 (55.2)	8.3 (8.3)	3.1 (3.2)
C_{16}-3-Mepy	57.0 (57.0)	8.7 (8.7)	3.0 (3.0)
C_{18}-3-Mepy	58.4 (58.6)	9.0 (9.0)	2.9 (2.9)
C_{12}-4-Mepy	51.8 (53.1)	7.9 (7.9)	3.5 (3.4)
C_{14}-4-Mepy	55.3 (55.2)	8.4 (8.3)	3.1 (3.2)
C_{16}-4-Mepy	57.0 (57.0)	8.8 (8.7)	3.0 (3.0)
C_{18}-4-Mepy	58.9 (58.6)	9.3 (9.0)	2.7 (2.9)

Table 2 Crystal parameters for [$C_{12}H_{25}$-mim][PF_6]

Formula	$C_{16}H_{31}F_6N_2P$
Formula weight	396.40
Crystal system	Monoclinic
Space group	$P2_1/a$
a/Å	9.175(2)
b/Å	9.849(3)
c/Å	22.197(4)
β/°	94.132(18)
U/Å^3	2000.7(8)
Z	4
D_c/g cm^{-3}	1.32
Crystal size/mm	$0.70 \times 0.40 \times 0.05$
Crystal description	Colourless plate
μ/mm^{-1}	0.192
2θ range/°	5 to 53
R_{merge}	0.037
No. of reflections measured	4676
Unique data	4401
Observed data	2497
No. of parameters	227
Absorption range	0.94–1.00
R, R_w	0.0394, 0.0436
S	1.339
Max. $\Delta\rho$/e Å^{-3}	0.219
Min. $\Delta\rho$/e Å^{-3}	−0.235

achieved by recrystallisation from methanol. Using this method, the only by-product is hydrochloric acid, which remains in the aqueous solution. These salts are thus guaranteed to be free of any traces of metal ions. Residual halide ions were removed by extended washing with water. Contamination of low melting salts containing anions such as $[BF_4]^-$ and $[CH_3CO_2]^-$ has been a problem due to the requirement to use metal salts, typically silver and lead respectively, in their preparation.[24,25]

None of the salts containing alkyl chains shorter than C_{12} display liquid crystalline behaviour.[26] The presence and temperature range of liquid crystallinity proved to vary greatly with different cations, and so each cation will be discussed separately. The data referred to in the following sections are collected in Table 3. In general the behaviour on cooling was very similar to that observed on heating, except that solidification points were always lower in temperature than melting points, thus giving larger mesophase ranges for the cooling cycles. The value of the solidification point was very dependent on the cooling rate employed. Therefore, only data recorded on heating cycles are reported except for the few examples where monotropic mesophases were observed, which are recorded in parentheses in Table 3. The mesophases observed were identified using POM and DSC. For all of the mesomorphic examples, a single enantiotropic smectic mesophase was observed, except for the methylpyridinium salts [C_{16}-3-Mepy][PF_6], [C_{16}-4-Mepy][PF_6] and [C_{18}-4-Mepy][PF_6], where the phase is only observed monotropically. Characteristic POM textures obtained on cooling of isotropic liquids are shown in Fig. 2 for [C_{16}-mim][PF_6] and [C_{16}-py][PF_6]. These textures are typical of those observed, which in all cases showed spontaneous formation of homeotropic domains with the optical axis perpendicular to the slide.[27] In the POM of [C_{16}-mim][PF_6] [Fig. 2(a)], small but characteristic focal conic textures can also be seen in the dark homeotropic regions. The similarity of the textures observed for [R-mim]$^+$ and [R-py]$^+$ salts indicates that the same type of mesophase

Table 3 Summary of DSC data and polarising microscope measurements obtained for [Q][PF_6] salts under study[a]

$[Q]^+$	T/°C	Energy/kJ mol^{-1}	Transition
C_{12}-mim	60	27.3	C→I
C_{14}-mim	74	30.9	C→S_A
	77	0.4	S_A→I
C_{16}-mim	75	37.5	C→S_A
	125	0.5	S_A→I
C_{18}-mim	80	43.8	C→S_A
	165	1.1	S_A→I
C_{12}-py	49	6.2	C→C_1
	89	3.9	C_1→C_2
	104	22.4[b]	C_2→C_3
	106	22.4[b]	C_3→I
C_{14}-py	53	5.8	C→C_1
	103	4.0	C_1→C_2
	109	16.5	C_2→C_3
	124	9.6	C_3→I
C_{16}-py	(86)	(−4.9)	
	104 (98)	27.7 (−20.9)	C→C_1
	126	8.4	C_1→S_A
	138	0.8	S_A→I
C_{18}-py	(89)	(−3.6)	
	107 (102)	32.3 (−22.2)	C→C_1
	126	7.6	C_1→S_A
	176	1.2	S_A→I
C_{12}-3-Mepy	55	28.2	C→I
C_{14}-3-Mepy	68	25.8	C→I
C_{16}-3-Mepy	(58)	(−35.9)	(S_A→C)
	74 (61)	36.0 (−0.5)	C→I (I→S_A)
C_{18}-3-Mepy	87	38.0	C→S_A
	94	0.5	S_A→I
C_{12}-4-Mepy	56	20.3	C→I
C_{14}-4-Mepy	71	28.1	C→I
C_{16}-4-Mepy	(55)	(−34.8)	(S_A→C)
	75 (60)	36.7 (−1.1)	C→I (I→S_A)
C_{18}-4-Mepy	(77)	(−41.8)	(S_A→C)
	88 (84)	33.6 (−0.4)	C→I (I→S_A)

[a]The entries in parentheses indicate transitions observed on cooling where these are significantly different from those observed on heating. [b]Peaks were not fully resolved, so individual transition enthalpies would not be recorded.

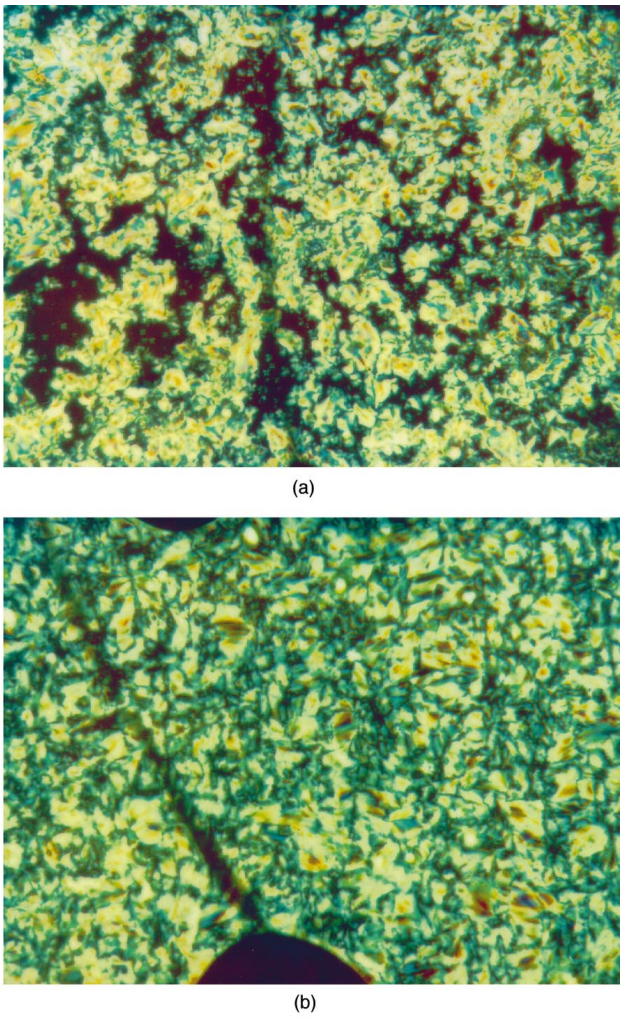

Fig. 2 Textures observed using POM (100× magnification) of (a) [C_{16}-mim][PF_6] at 98 °C, and (b) [C_{16}-py][PF_6] at 121 °C. Both photographs were taken after cooling from the isotropic phase.

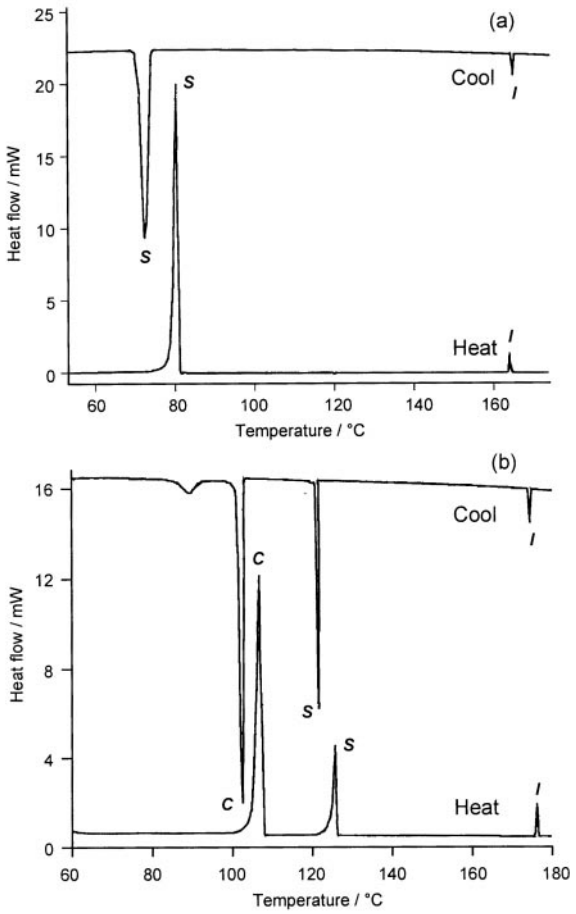

Fig. 3 DSC traces observed on heating and cooling of (a) [C_{18}-mim][PF_6], and (b) [C_{18}-py][PF_6]. The peak labels indicate the type of phase transition occurring: C = solid ↔ solid; S = solid ↔ smectic; I = smectic ↔ isotropic. Heating and cooling rates of 10 °C min^{-1} were employed.

is observed for both materials. The textures shown are typical for all salts that displayed liquid crystalline behaviour. In light of the evidence of the POM observations, the mesophases are assigned as smectic A (S_A). Further support for the assignment of a smectic A mesophase comes from the fact that the $[PF_6]^-$ salts displayed contact miscibility in the liquid crystalline state with the corresponding $[CoCl_4]^{2-}$ analogues. For these studies small amounts of the two different salts were placed slightly apart between two cover slips. The samples were heated on the microscope heating stage to above their melting points and then rapidly cooled to avoid excessive mixing. Further heating and cooling resulted in the observation of a uniform mesophase across the meeting point of the two samples. Such behaviour is only observed when the same mesophase structure is present. DSC heating and cooling curves for [C_{18}-mim][PF_6] and [C_{18}-py][PF_6] are illustrated in Fig. 3, from which it can be seen that the transition from the solid to the liquid crystalline phase was of much higher energy than the transition from the liquid crystal to the isotropic liquid.

(i) 1-Alkyl-3-methylimidazolium salts

The dodecyl-substituted salt showed no mesomorphic behaviour either on heating or cooling, while all the other salts displayed enantiotropic mesophases. The melting and clearing points are displayed graphically in Fig. 4(a). The close agreement between the clearing point on heating and the point at which the mesophase reforms on cooling is further evidence for the purity of the salts. The melting points of the salts

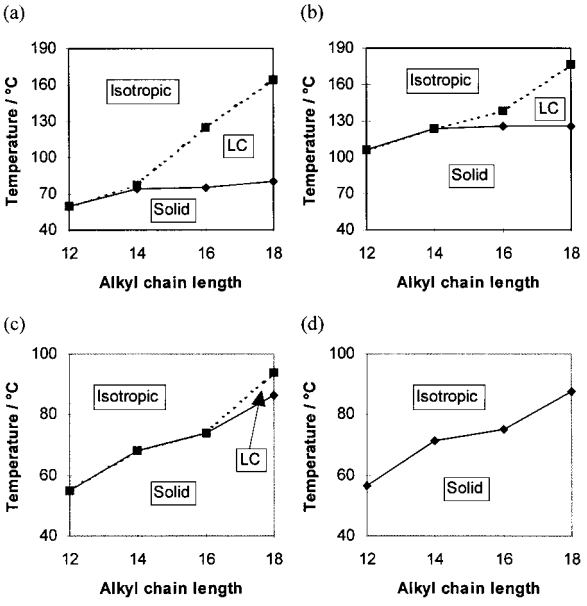

Fig. 4 Plots showing the melting and clearing temperatures observed on heating of (a) [C_n-mim][PF_6], (b) [C_n-py][PF_6], (c) [C_n-3-Mepy][PF_6], and (d) [C_n-4-Mepy][PF_6].

increased only slightly with increasing alkyl chain length, while the clearing point increased markedly, ultimately giving a mesophase temperature range of 84 °C on heating and 93 °C on cooling for the octadecyl substituted salt. Thus, the liquid crystalline range increased greatly with increasing alkyl chain length.

(ii) 1-Alkylpyridinium salts

No mesomorphic behaviour was observed for either the C_{12}- or $[C_{14}\text{-py}]^+$ salts. The melting points of all $[\text{R-py}]^+$ salts were higher than those of the equivalent $[\text{R-mim}]^+$ salts, concurring with observations made previously for ionic liquids based on such cations.[29] The longer chain salts (C_{16}, C_{18}) did display mesomorphic behaviour, and as was the case with the $[\text{R-mim}]^+$ salts the clearing temperature increased greatly on increasing the alkyl chain length by only two carbon atoms. In contrast, the melting point only increased from 124 to 126 °C on increasing the alkyl chain length from 14 to 18. The melting and clearing points of these species are displayed graphically in Fig. 4(b). Unlike the $[\text{R-mim}]^+$ salts, however, solid phase transitions were observed at temperatures below the melting point in all of the $[\text{R-py}]^+$ salts studied. It can be seen from Table 3 that the solid phase behaviour is quite different for the two non-liquid crystalline salts (C_{12} and C_{14}) compared with those which do display liquid crystalline behaviour (C_{16} and C_{18}). In the latter case only one solid–solid phase transition was observed on heating and two on cooling, as shown in Fig. 3(b), while in the former there were three transitions both on heating and cooling.

(iii) 1-Alkyl-3-methylpyridinium salts

3-Methylpyridinium is a more bulky headgroup than the simple pyridinium ring; this was expected to give the dual effects of lowering the melting points and reducing the tendency towards mesomorphic behaviour. This proved indeed to be the case, with the C_{16} salt only displaying a liquid crystalline phase on cooling (monotropic behaviour), and over a temperature range of just 3 °C. The C_{18} salt, however, shows enantiotropic behaviour over a temperature range of *ca.* 10 °C. This information, and the behaviour observed for the shorter chain salts, is summarised in Table 3 and Fig. 4(c). The C_{12} and C_{14} salts display no mesomorphism, and simply melt directly to the isotropic liquid. Unlike the pyridinium salts, there are no solid–solid phase transitions.

(iv) 1-Alkyl-4-methylpyridinium salts

As was the case for the $[\text{R-3-Mepy}]^+$ salts discussed above, the presence of a 4-methyl substituent on the pyridinium ring resulted in a lowering of the melting point and a reduction in the stability of the mesophase relative to the equivalent pyridinium salt. In this case, both the C_{16} and C_{18}-substituted salts displayed only monotropic smectic phases, while the C_{12} and C_{14} salts showed no mesophases. The other information is collected in Table 3 and Fig. 4(d). These data show that the melting points for each alkyl chain length are almost identical to the analogous $[\text{R-3-Mepy}]^+$ salt. A further feature in common with the $[\text{R-3-Mepy}]^+$ salts was the absence of phase transitions in the solid phase.

Characterisation

Characterisation of the anhydrous salts was largely straightforward, being carried out initially using CHN analysis, ^{1}H NMR and IR spectroscopy. CHN analytical data for all salts prepared are summarised in Table 1, all being satisfactory except for $[C_{12}\text{-4-Mepy}][PF_6]$, for which the carbon analysis was slightly low. This salt had proved very troublesome to purify satisfactorily by recrystallisation as an oil formed on dissolving the crude solid in methanol. It is possible, therefore, that the melting point recorded (55 °C) was slightly low due to the presence of trace amounts of impurities, although no impurity peaks could be seen in the ^{1}H NMR spectrum. ^{1}H NMR spectroscopy provided a convenient method for confirming the purity of the cation, and that no solvent residues remained in the salts. The IR spectra simply allowed confirmation of the presence of both the appropriate cation and the $[PF_6]^-$ anion in the salts prepared. The anion displays a characteristic strong peak at 830 cm^{-1}.

Positive ion FAB mass spectrometry provided a convenient method for unequivocal characterisation of the salts. All of the data are collected in Table 4. Although the most intense peak was the isolated cation, the next most intense peak generally corresponded to the species $\{[Q]_2[PF_6]\}^+$ (Q = organic cation). The intensity of such peaks was typically *ca.* 5% that of the Q^+ peak, with the intensity generally greater for the shorter chain salts. This type of clustering phenomenon has been observed before in similar organic cation salts.[30] The data for $[C_{18}\text{-mim}][PF_6]$ was slightly different, with the second most intense mass peak occurring at $m/z = 574$ (m/z for $\{[C_{18}\text{-mim}]_2[PF_6]\}^+$ is expected at 816). This may correspond with the species $\{[C_{18}\text{-mim}]_3[PF_6]\}^{2+}$ (expected $m/z = 575$), although why such a species is only observed for this salt is unclear.

The crystal structure of $[C_{12}\text{-mim}][PF_6]$

All of the salts investigated were crystalline, and in the case of $[C_{12}\text{-mim}][PF_6]$ it proved possible to produce crystals of sufficient quality for single crystal X-ray diffraction. This is the first long chain 1-alkyl-3-methylimidazolium salt whose crystal structure has been reported, although the structure of 1,3-didodecylbenzimidazolium chloride was reported recently.[21] The only other related salt for which a crystal structure has been determined is 1-ethyl-3-methylimidazolium hexafluorophosphate.[31] The much shorter alkyl chain in this species means that the structure is quite different from that reported here. Furthermore, almost all other amphiphilic salts for which crystal structures have been determined are simple halide salts, and this is one of the first containing a $[PF_6]^-$ anion.

The crystal structure of $[C_{12}H_{25}\text{-mim}][PF_6]$ consists of discrete cations (Fig. 5) and anions separated by at least van der Waals distances (see Fig. 6). The closest contact is 2.950(3) Å for F(2)···C(2)*, (*$x-1$, y, z). Selected geometric parameters are given in Table 5 and all are close to the expected values. The imidazolium ring is completely planar, within experimental error, and the bond lengths are very close to those observed in other 1-alkyl-3-methylimidazolium salts.[32] The straight chain nature of the alkyl group is disrupted close to the ring where it adopts a bent conformation, as shown by the torsion angles N(2)–C(5)–C(6)–C(7), C(5)–C(6)–C(7)–C(8) and C(6)–C(7)–C(8)–C(9) of −66.7(3), 176.4(2) and 60.2(3)° respectively. All other carbon chain torsion angles approach 180°. The chain configuration and the lack of any disorder in the structure appear to be a consequence of the interdigitated molecular packing. The twist in the alkyl chain occurs over a larger number of carbon atoms than is observed in the $[(C_{12}H_{25})_2\text{-benzimidazolium}]Cl$ salt. The cation in the latter has a geometry described as being like a 'two-legged stool',[21] whereas the $[C_{12}H_{25}\text{-mim}]^+$ cation could be described as having a spoon-shaped structure, as illustrated in Fig. 5. The X-ray powder diffraction pattern for the $[C_{12}H_{25}\text{-mim}][PF_6]$ showed the same unit cell and confirms that the single crystal is typical of the bulk synthetic sample.

The crystal structure of the salt was similar to that of liquid crystalline alkylammonium and alkylpyridinium salts reported previously.[33,34] It consists of sheets of imidazolium rings and hexafluorophosphate ions, separated by interdigitated alkyl chains; the unit cell is shown in Fig. 6, while Fig. 7

Table 4 Peaks observed in the positive ion mass spectra of $[R\text{-mim}]^+$, $[R\text{-py}]^+$, $[R\text{-3-Mepy}]^+$ and $[R\text{-4-Mepy}]^+$ salts of $[PF_6]^-$

Salt	*m/z* (relative intensity)	Assignment
$[C_{12}H_{25}\text{-mim}][PF_6]$	251 (100)	$[C_{12}H_{25}\text{-mim}]^+$
	648 (14)	$\{[C_{12}H_{25}\text{-mim}]_2[PF_6]\}^+$
$[C_{14}H_{29}\text{-mim}][PF_6]$	279 (100)	$[C_{14}H_{29}\text{-mim}]^+$
	704 (6)	$\{[C_{14}H_{29}\text{-mim}]_2[PF_6]\}^+$
$[C_{16}H_{33}\text{-mim}][PF_6]$	307 (100)	$[C_{16}H_{33}\text{-mim}]^+$
	760 (3)	$\{[C_{16}H_{33}\text{-mim}]_2[PF_6]\}^+$
$[C_{18}H_{37}\text{-mim}][PF_6]$	335 (100)	$[C_{18}H_{37}\text{-mim}]^+$
	574 (7)	$\{[C_{18}H_{37}\text{-mim}]_3[PF_6]\}^{2+}$
	816 (1.5)	$\{[C_{18}H_{37}\text{-mim}]_2[PF_6]\}^+$
$[C_{12}H_{25}\text{-py}][PF_6]$	248 (100)	$[C_{12}H_{25}\text{-py}]^+$
	642 (10)	$\{[C_{12}H_{25}\text{-py}]_2[PF_6]\}^+$
$[C_{14}H_{29}\text{-py}][PF_6]$	276 (100)	$[C_{14}H_{29}\text{-py}]^+$
	698 (6)	$\{[C_{14}H_{29}\text{-py}]_2[PF_6]\}^+$
$[C_{16}H_{33}\text{-py}][PF_6]$	304 (100)	$[C_{16}H_{33}\text{-py}]^+$
	754 (4)	$\{[C_{16}H_{33}\text{-py}]_2[PF_6]\}^+$
$[C_{18}H_{37}\text{-py}][PF_6]$	332 (100)	$[C_{18}H_{37}\text{-py}]^+$
	809 (4)	$\{[C_{18}H_{37}\text{-py}]_2[PF_6]\}^+$
$[C_{12}H_{25}\text{-3-Mepy}][PF_6]$	262 (100)	$[C_{12}H_{25}\text{-3-Mepy}]^+$
	670 (7)	$\{[C_{12}H_{25}\text{-3-Mepy}]_2[PF_6]\}^+$
$[C_{14}H_{29}\text{-3-Mepy}][PF_6]$	290 (100)	$[C_{14}H_{29}\text{-3-Mepy}]^+$
	726 (9)	$\{[C_{14}H_{29}\text{-3-Mepy}]_2[PF_6]\}^+$
$[C_{16}H_{33}\text{-3-Mepy}][PF_6]$	318 (100)	$[C_{16}H_{33}\text{-3-Mepy}]^+$
	782 (3.5)	$\{[C_{16}H_{33}\text{-3-Mepy}]_2[PF_6]\}^+$
$[C_{18}H_{37}\text{-3-Mepy}][PF_6]$	346 (100)	$[C_{18}H_{37}\text{-3-Mepy}]^+$
	837 (3.5)	$\{[C_{18}H_{37}\text{-3-Mepy}]_2[PF_6]\}^+$
$[C_{12}H_{25}\text{-4-Mepy}][PF_6]$	262 (100)	$[C_{12}H_{25}\text{-4-Mepy}]^+$
	670 (6)	$\{[C_{12}H_{25}\text{-4-Mepy}]_2[PF_6]\}^+$
$[C_{14}H_{29}\text{-4-Mepy}][PF_6]$	290 (100)	$[C_{14}H_{29}\text{-4-Mepy}]^+$
	726 (8)	$\{[C_{14}H_{29}\text{-4-Mepy}]_2[PF_6]\}^+$
$[C_{16}H_{33}\text{-4-Mepy}][PF_6]$	318 (100)	$[C_{16}H_{33}\text{-4-Mepy}]^+$
	782 (3.5)	$\{[C_{16}H_{33}\text{-4-Mepy}]_2[PF_6]\}^+$
$[C_{18}H_{37}\text{-4-Mepy}][PF_6]$	346 (100)	$[C_{18}H_{37}\text{-4-Mepy}]^+$
	837 (5)	$\{[C_{18}H_{37}\text{-4-Mepy}]_2[PF_6]\}^+$

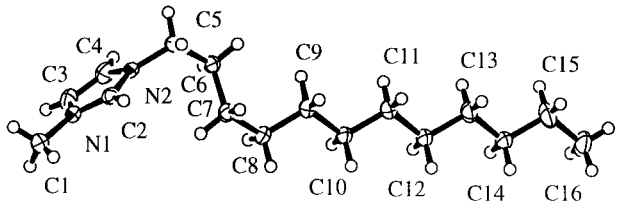

Fig. 5 Structure of the unique 1-dodecyl-3-methyl cation in $[C_{12}\text{-mim}][PF_6]$.

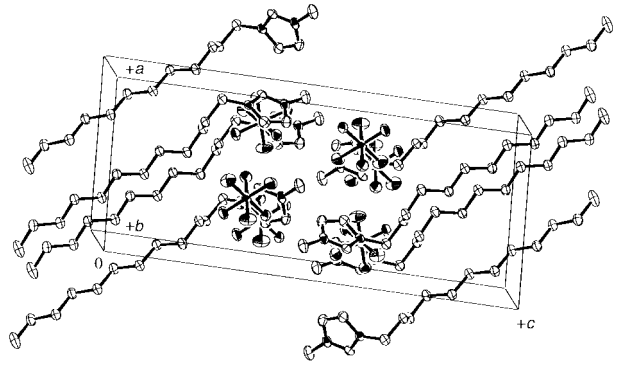

Fig. 6 Unit cell of $[C_{12}\text{-mim}][PF_6]$.

demonstrates the interdigitated pattern. Of note is the stepped structure, with the alkyl chains tilted relative to the layers of cations and anions. The spacing between each layer was 22.197(4) Å.

The closest cation C(2)···F–PF_5 contact (2.950 Å) is slightly shorter than the analogous closest contact taken from the crystal structure of the short chain 1-ethyl-3-methylimidazolium hexafluorophosphate salt (3.206 Å).[31] However, in both cases, the contacts are close to the van der Waals distance and interactions appear to be largely coulombic. This is consistent with earlier work which has shown that hydrogen-bonding is not observed in these and related systems when the charge density (ρ) on the halide atoms of the anion is <1, following the relation $\rho = z^2/x$ where z is the overall charge on the ion and x is the number of halide atoms in the complex.[35]

Powder X-ray diffraction studies

Powder X-ray diffraction studies were carried out on all of the salts in order to gain further structural information. In all cases, the peak with the lowest value of 2θ displayed the highest intensity. The *d*-spacing calculated from this peak increased relatively regularly with increasing alkyl chain length, as listed in Table 6. In addition, for each class of cation the patterns obtained were similar for all alkyl chain lengths, although with different values of 2θ. Thus all salts for each cation are isostructural. These data also indicate that the structures in all cases involve intercalated layers of cations as found for the structure of $[C_{12}H_{25}\text{-mim}][PF_6]$ discussed above, with a layer spacing corresponding to the lowest angle peak. The very small values of 2θ for these peaks mean that there is some margin for error in the layer separation values obtained, owing to limits in the resolution of the diffractometer employed. Assuming that the values are correct to $\pm 0.025^\circ$, the layer separations can be regarded as accurate to ± 0.3 Å. Thus the layer separation calculated from powder X-ray diffraction data for $[C_{12}H_{25}\text{-mim}][PF_6]$ (22.4 Å) is equivalent to that obtained from the single crystal data [22.197(4) Å], to within experimental error.

Mixtures of salts—binary systems

In an attempt to reduce the melting point of the salts, preferably without decreasing their liquid crystalline temperature range, an investigation of the effect of mixing the salts $[C_{16}\text{-mim}][PF_6]$ and $[C_{16}\text{-py}][PF_6]$ was carried out. Such

Table 5 Selected interatomic distances (Å) and torsion angles (°) for X

N(1)–C(1)	1.468(3)	N(1)–C(2)	1.322(3)
N(1)–C(3)	1.373(3)	N(2)–C(2)	1.326(3)
N(2)–C(4)	1.374(3)	N(2)–C(5)	1.477(3)
C(3)–C(4)	1.334(4)		
P(1)–F(1)	1.591(2)	P(1)–F(2)	1.610(2)
P(1)–F(3)	1.593(2)	P(1)–F(4)	1.602(2)
P(1)–F(5)	1.584(2)	P(1)–F(6)	1.599(2)
N(2)C(5)C(6)C(7)	−66.7(3)	C(2)N(2)C(5)C(6)	112.4(2)
C(4)N(2)C(5)C(6)	−66.5(3)	C(5)C(6)C(7)C(8)	176.4(2)
C(6)C(7)C(8)C(9)	60.2(3)	N(2)C(2)N(1)C(1)	−176.8(2)

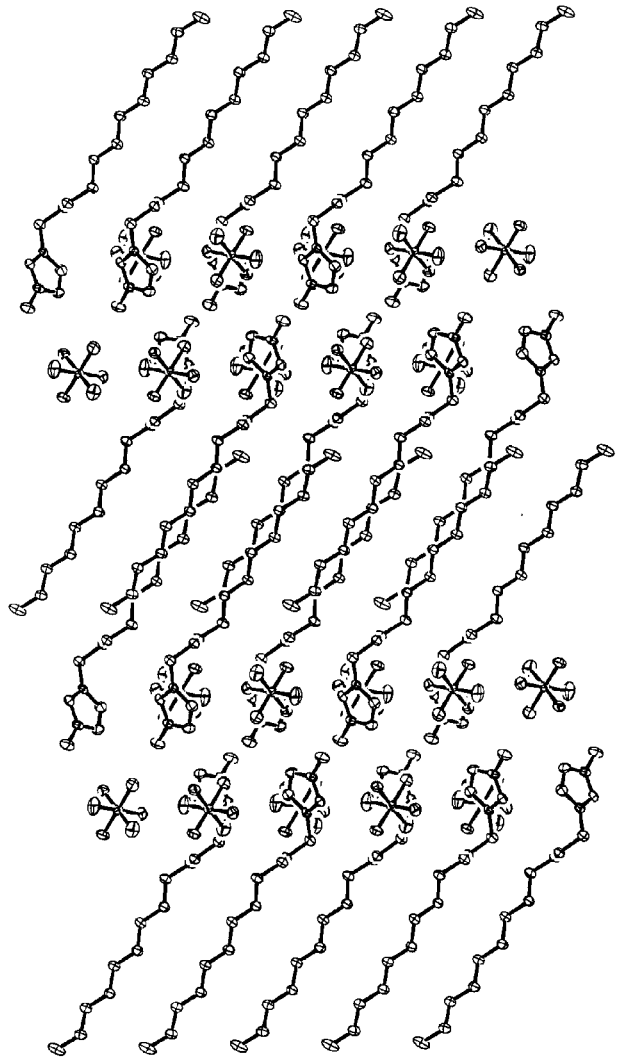

Fig. 7 Overall structure of $[C_{12}\text{-mim}][PF_6]$ showing the interdigitation and the tilted alkyl chains.

methods are routinely used to lower the melting point of both molten salts and molecular liquid crystalline materials, by the formation of eutectic mixtures. The mixtures were prepared by grinding together various proportions of the two constituents, followed by melting, re-cooling, and grinding again. This procedure was repeated three times, by which stage it was assumed that a homogeneous mixture had been prepared.

The melting and clearing points of the binary systems were then investigated by POM and DSC. In all cases a mesophase was observed which was of the same type as that of the individual components, and in no cases was biphasic behaviour observed. The data obtained are summarised in Fig. 8 and Table 7, where it can be seen that although the clearing point varied smoothly as the composition was changed, the melting point varied little between pure $[C_{16}\text{-mim}][PF_6]$ and the 75% $[C_{16}\text{-mim}][PF_6]$–25% $[C_{16}\text{-py}][PF_6]$ mixture. Thus, this mixture has a larger mesophase range (55 °C) than that of the pure $[C_{16}\text{-mim}][PF_6]$ (49 °C). It should also be noted that the melting transition for the mixed salts was not a sharp transition as observed for the pure salts, but was spread over a range of several degrees. This was reflected in broad peaks in the DSC traces obtained for the 50%–50% and 25% $[C_{16}\text{-mim}][PF_6]$–75% $[C_{16}\text{-py}][PF_6]$ mixtures. It was disappointing that no depression in the melting point was observed, although this may be a reflection of the similarity in the structure of the cations.

One additional benefit of carrying out the studies on the mixed salts, however, is that it allowed confirmation of the fact that the mesophase formed was the same for the $[R\text{-mim}]^+$ and the $[R\text{-py}]^+$ salts. This arises from the 'miscibility

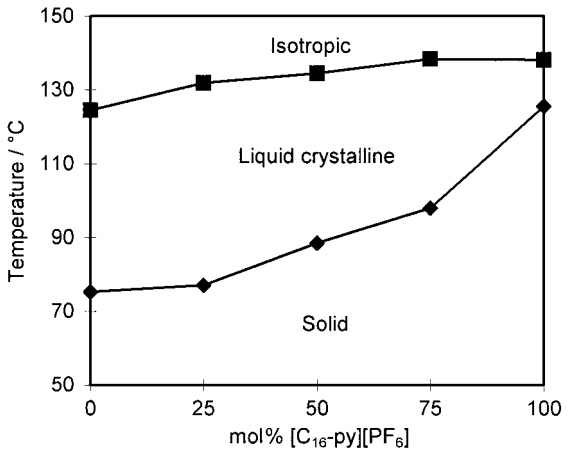

Fig. 8 Plot showing the variation in melting and clearing point on heating salts prepared from various proportions of $[C_{16}\text{-mim}][PF_6]$ and $[C_{16}\text{-py}][PF_6]$.

Table 6 Layer separations obtained from powder X-ray diffraction measurements

	Layer separation/Å			
Chain length (*n*)	$[R\text{-mim}]^+$	$[R\text{-py}]^+$	$[R\text{-3-Mepy}]^+$	$[R\text{-4-Mepy}]^+$
12	22.4	22.2	23.5	23.0
14	24.2	23.9	25.9	24.9
16	26.5	26.2	27.4	27.1[a]
18	27.7	27.4	29.1	27.4

[a]Poor quality data.

Table 7 Transitions observed in on heating mixtures of $[C_{16}\text{-mim}][PF_6]$ and $[C_{16}\text{-py}][PF_6]$, and transition energies obtained from DSC measurements

mol% $[C_{16}\text{-py}][PF_6]$	T/°C	ΔH^a/kJ mol^{-1}	Transition
100	104	27.7	C→C_1
	126	8.4	C_1→S
	138	0.8	S→I
75	72	32.5[b]	C→C_1
	98		C_1→S
	138	0.7	S→I
50	76	31.1[b]	C→C_1
	89		C_1→S
	135	0.8	S→I
25	77	32.2	C→S
	132	0.7	S→I
0	75	37.5	C→S
	125	0.5	S→I

[a]Calculated using an averaged molecular mass for the relative proportion of the two constituents. [b]Overlapping of peaks prevented calculation of individual transition enthalpies.

rule', which states that 'all liquid crystalline modifications which exhibit an uninterrupted series of mixed crystals in binary systems without contradiction can be marked with the same symbol'.[36]

Discussion

In general, with increasing alkyl chain length the melting points increased only modestly. In the case of the liquid crystalline $[R\text{-mim}]^+$ and $[R\text{-py}]^+$ salts, however, the clearing temperature increased dramatically with increasing chain length. The widest mesophase range was observed for the salt $[C_{18}H_{37}\text{-mim}][PF_6]$, from 80 to 165 °C on heating, with an even larger range on cooling (as was observed in all cases). The temperature at which texture was observed on cooling from the isotropic liquid (*i.e.* formation of a liquid crystalline phase) was almost identical to the clearing point in pure samples. The solidification temperature varied according to the rate of cooling employed, owing to the supercooling often observed for the mesophase–solid transition in liquid crystalline materials. The $[R\text{-3-Mepy}]^+$ and $[R\text{-4-Mepy}]^+$ salts displayed liquid crystalline behaviour only over very small temperature ranges, and for the C_{16} and C_{18} salts only. In the case of the $[R\text{-4-Mepy}]^+$ salts the mesophases were exclusively monotropic, while for the $[R\text{-3-Mepy}]^+$ salts the C_{16} salt displayed monotropic behaviour and the C_{18} salt enantiotropic behaviour.

The data in Table 3 clearly indicate that the enthalpy of melting (ΔH_{fus}) was always much larger than the enthalpy of the clearing transition (ΔH_{clear}). This is a common observation in thermotropic liquid crystals. The only other similar liquid crystalline $[PF_6]^-$ salt reported to date is $[(C_{16}H_{33})_2bzm][PF_6]$ (bzm = benzimidazolium). This forms a lamellar phase at 103.3 °C on cooling with an enthalpy of 2.0 kJ mol^{-1}, followed by solidification at 61.3 °C with an enthalpy of 46.1 kJ mol^{-1}.[21] The equivalent values for $[C_{16}\text{-mim}][PF_6]$ are the formation of a smectic phase at 122 °C with an enthalpy of 0.5 kJ mol^{-1}, and solidification at 62 °C with an enthalpy of 37.2 kJ mol^{-1}. Thus, the two long alkyl chains in the benzimidazolium salt result in a less stable mesophase than the single one in the $[C_{16}\text{-mim}]^+$ salt, although in the former case the transition enthalpy is somewhat higher. One noticeable observation from the DSC data was that the enthalpies of the melting (ΔH_{fus}) and clearing (ΔH_{clear}) transitions increased with increasing chain length. This suggests that chain interdigitation is of increasing importance in stabilising the mesophase as the chain length increases.

In the absence of variable temperature low-angle X-ray studies, the principle evidence for the mesophase structure comes from the textures observed using POM, as illustrated in Fig. 2. As has been stated in the previous section, these were broadly similar for all salts, and were typical of smectic A phases. Smectic A mesophases have previously been identified for other amphiphilic materials, for example $[C_n\text{-4-Mepy}]Br$ (n = 16, 18, 22) and $[C_{22}\text{-4-Mepy}]I$.[3,37]

Previous investigations of the thermal behaviour of salts with interdigitated structures suggest that formation of the liquid crystalline phases results from melting of the alkyl chains, while the ionic layers between remain ordered until the clearing point. X-Ray studies have shown that in many cases the layer separation actually decreases on moving from the crystalline solid to the smectic phase. For example, solid *n*-decylammonium chloride has a layer spacing of 28.1 Å in its solid phase, and 24.6 Å in its first smectic phase.[2] The Raman spectrum of the same compound shows clear signs of loss of order in the alkyl chains as the temperature is increased.[38]

It is possible that the tilted orientation of the alkyl chains relative to the unit cell observed in the crystal structure of $[C_{12}\text{-mim}][PF_6]$ gives a clue as to the structure of the mesophase in these systems. This solid state arrangement can be compared with the smectic C liquid crystal phase, as all of the alkyl chains are tilted at an angle of *ca.* 57° to the *ab* plane containing the anions and the cationic head groups. The thermodynamic ordering of liquid crystalline phases allows only the smectic A and nematic phases at higher temperatures than smectic C phases. The relatively large enthalpy (and thus entropy) change on melting indicates a considerable change in the structure of the system. Thus, it may be postulated that the mesophase structure involves conformational melting of the alkyl chains, accompanied by loss of the tilted orientation as indicated in Fig. 9, giving a smectic A phase. Further evidence can only be gained by use of variable temperature low angle X-ray studies of the salts, unavailable for this study.

The enthalpy of the smectic–isotropic transition in the $[R\text{-3-Mepy}]^+$ salts was much smaller than the value for the equivalent pyridinium salt, suggesting that the methyl group was lowering the stability of the mesophase. It is notable in this series that, unlike the $[R\text{-py}]^+$ salts, the melting point increases steadily through the series n = 12–18. Similar behaviour was noted for the $[R\text{-4-Mepy}]^+$ salts, although the mesophases observed for these compounds were monotropic in nature. Overall, the widest liquid crystalline ranges were observed for the $[R\text{-mim}]^+$ salts, followed by those for the $[R\text{-py}]^+$ salts, while the $[R\text{-3-Mepy}]^+$ and $[R\text{-4-Mepy}]^+$ salts showed the least tendency to form mesophases. A similar phenomenon was observed for liquid crystalline salts based on pyridinium and ethylpyridinium halide salts containing *N*-substituted mesogenic groups.[7] It is clear that the $[R\text{-mim}]^+$ salts, whose liquid crystalline behaviour has been little studied to date, present considerable advantages compared with the pyridinium salts for future development in this area.

One intriguing observation, which can be seen from the data in Table 3, was that all of the pyridinium salts displayed solid phase polymorphism at temperatures below the melting point. None of the other salts displayed this phenomenon. There was a noticeable difference between the non-liquid crystalline C_{12} and C_{14} salts, which displayed three transitions below their melting point both on heating and cooling, and the liquid crystalline C_{16} and C_{18} salts which displayed just one transition before melting, and two transitions on cooling. These transitions have been shown to appear consistently on repeated heat–cool cycles, indicating that they are not simply artefacts. In the case of the C_{16} and C_{18} salts, the lowest temperature solid phase transition was of much higher enthalpy than the higher temperature one. This suggested that a large degree of disorder was occurring in the first transition, presumably with the formation of a solid of structure more similar to that of the liquid crystalline phase. Clearly variable temperature powder X-ray diffraction or vibrational spectroscopic

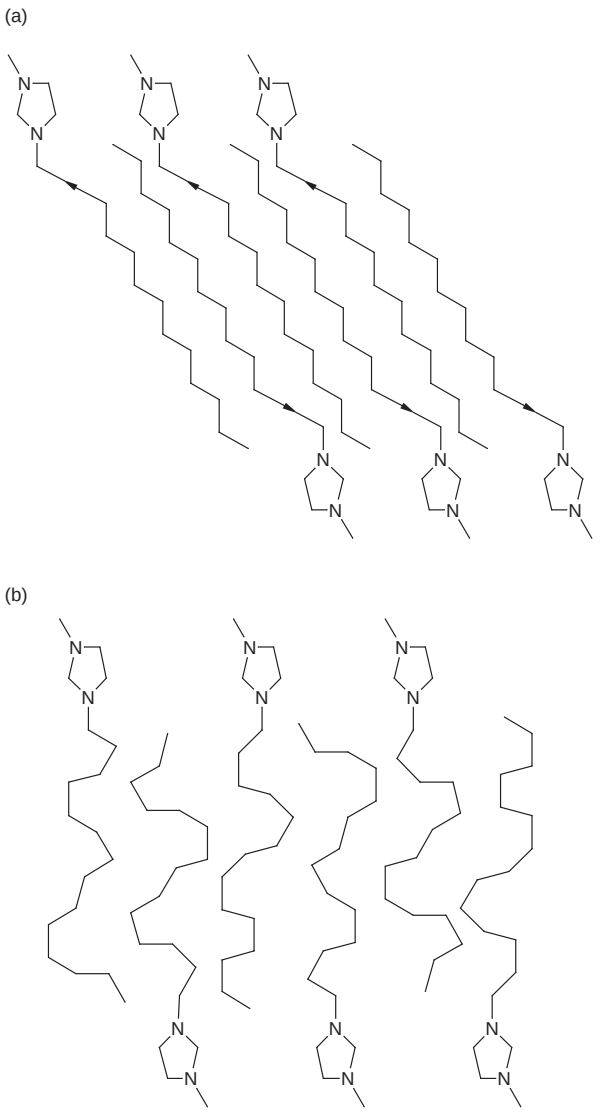

Fig. 9 Schematic representation of (a) the cation structure in the solid state of the mim salts, and (b) a possible cation structure of the smectic A phase, showing the effect of conformational melting of the alkyl chains. $[PF_6]^-$ ions have been omitted for clarity.

studies would help elucidate any changes of structure. Such information might also provide valuable information on the structure of the liquid crystalline phases. Behaviour of this type has been noted previously for liquid crystalline pyridinium salts with dodecyl sulfate anions, although the authors also did not attempt to explain the phenomenon.[14]

Conclusions

In this paper we have described the properties of a series of novel hexafluorophosphate salts, many of which display liquid crystalline properties on melting. The salts are closely related to ionic liquids which are finding increasing use as reaction solvents. They may be prepared very easily, and unlike many ionic liquids are insoluble in water. It is clear that cations based on the imidazolium ring give materials with much larger mesophase ranges for a given alkyl chain length, compared with the equivalent pyridinium salts. The existence or not of a mesophase is extremely dependent both on the structure of the cationic head group and the length of the alkyl substituent. In general, however, the longer the alkyl chain the more stable the mesophase formed. In the case of the nine salts which did display liquid crystalline behaviour, only a single mesophase was formed in each case, which is in common with the analogous Cl^-, $[CoCl_4]^{2-}$ and $[NiCl_4]^{2-}$ salts.[12] The textures observed using POM were very similar, and were interpreted as indicating formation of a smectic A mesophase.

The salts based on the pyridinium cation displayed higher melting points and smaller mesophase ranges than imidazolium salts of equivalent alkyl chain length. The pyridinium salts displayed interesting polymorphism, however, with phase transitions observed at temperatures below the melting points of the salts. Both this phenomenon and the structures of the smectic A mesophases would merit further investigation using variable temperature small angle X-ray techniques unavailable in the present study. Substitution of the pyridinium ring at the 3- and 4-positions with methyl groups reduced the melting points of the salts, but reduced the tendency to form liquid crystalline phases still further.

Mixtures formed by combining salts with imidazolium and pyridinium cations did not result in depression of the melting point below that of the pure imidazolium salt. A slightly larger mesophase range was obtained for one of the mixtures, suggesting that further investigations, perhaps with cations of greater structural difference, might yield interesting results.

The intention in future studies is to investigate how the mesophase range and stability are affected by use of a mesogenic substituent in place of the simple alkyl chains. It is hoped that such a modification will increase the stability of the mesophase, important in any application, without significantly increasing the melting point of the salts. We also hope to extend the range of anions employed to investigate the effect this has on mesophase formation.

Acknowledgements

We would like to thank Dr John Liggat, Margaret Adams and the Queen's University of Belfast School of Chemistry analytical services for assistance with DSC measurements and CHN analysis; Dr Cecil Burdett and Mark Nieuwenhuyzen for assistance with powder X-ray diffraction studies; the mass spectrometry services of the University of Strathclyde and the Queen's University of Belfast. We would also like to thank the University of Strathclyde (C.M.G. and A.R.K.), the ERDF Technology Development Programme and the QUESTOR Centre (J.D.H.) for financial support, and the EPSRC and Royal Academy of Engineering for the award of a Clean Technology Fellowship (to K.R.S.).

References

1 A. Skoulios and V. Luzzati, *Acta Crystallogr.*, 1961, **14**, 278.
2 See, *e.g.*: V. Busico, P. Cernicchiaro, P. Corradini and M. Vacatello, *J. Phys. Chem.*, 1983, **87**, 1631.
3 See, *e.g.*: C. G. Bazuin, D. Guillon, A. Skoulios and J.-F. Nicoud, *Liq. Cryst.*, 1986, **1**, 181.
4 J. J. H. Nusselder, J. B. F. N. Engberts and H. A. van Doren, *Liq. Cryst.*, 1993, **13**, 213.
5 Y. Kosaka, T. Kato and T. Uryu, *Liq. Cryst.*, 1995, **18**, 693.
6 S. Ujiie and K. Iimura, *Chem. Lett.*, 1990, 995.
7 D. Navarro-Rodriguez, Y. Frere, P. Gramain, D. Guillon and A. Skoulios, *Liq. Cryst.*, 1991, **9**, 321; E. Bravo-Grimaldo, D. Navarro-Rodriguez, A. Skoulios and D. Guillon, *Liq. Cryst.*, 1996, **20**, 393.
8 Y. Z. Yousif, A. A. Othman, W. A. Al-Masoudi and P. R. Alapati, *Liq. Cryst.*, 1992, **12**, 363.
9 Y. Haramoto, S. Ujiie and M. Nanasawa, *Liq. Cryst.*, 1996, **21**, 923.
10 Y. Kosaka, T. Kato and T. Uryu, *Liq. Cryst.*, 1995, **18**, 693.
11 F. Neve, *Adv. Mater.*, 1996, **8**, 277.
12 K. R. Seddon, C. J. Bowlas and D. W. Bruce, *Chem. Commun.*, 1996, 1625.
13 V. Busico, D. Castaldo and M. Vacatello, *Mol. Cryst. Liq. Cryst.*, 1981, **78**, 221.
14 D. W. Bruce, S. Estdale, D. Guillon and B. Heinrich, *Liq. Cryst.*, 1995, **19**, 301.
15 S. Ujiie and K. Iimura, *Chem. Lett.*, 1994, 17.

16 K. R. Seddon in *Proceedings of the 5th International Symposium on Molten Salt Chemistry and Technology*, ed. H. Wendt, Trans Tech Publications Ltd., Uetikon–Zürich, 1998, p. 53.
17 P. Bonhôte, A.-P. Dias, N. Papageorgiou, K. Kalyanasundaram and M. Grätzel, *Inorg. Chem.*, 1996, **35**, 1168.
18 Y. Chauvin, L. Mussmann and H. Olivier, *Angew. Chem., Int. Ed. Engl.*, 1995, **34**, 2698.
19 R. Mukkamala, C. L. Burns, R. M. Catchings and R. G. Weiss, *J. Am. Chem. Soc.*, 1996, **118**, 9498 and references therein.
20 H. Kansui, S. Hiraoka and T. Kunieda, *J. Am. Chem. Soc.*, 1996, **118**, 5346 and references therein.
21 K. M. Lee, C. K. Lee and J. B. Lin, *Chem. Commun.*, 1997, 899.
22 M. C. Burla, M. Camalli, G. Cascarano, C. Giacovazzo, G. Polidori, R. Spagna and D. Viterbo, *J. Appl. Crystallogr.*, 1989, **22**, 389.
23 TeXsan: Single Crystal Structure Analysis Software, Version 1.6. Molecular Structure Corporation, The Woodlands, TX 77381, 1993.
24 J. S. Wilkes and M. J. Zaworotko, *J. Chem. Soc., Chem. Commun.*, 1992, 965.
25 B. Ellis, personal communication.
26 C. M. Gordon, J. D. Holbrey and K. R. Seddon, unpublished work.
27 D. Demus and L. Richter, *Textures of Liquid Crystals*, Verlag Chemie, Weinheim, 1978, p. 61.
28 G. W. Gray and J. W. Goodby, *Smectic Liquid Crystals, Textures and Structures*, Leonard Hill, Glasgow, 1984.
29 J. S. Wilkes, J. A. Levisky, R. A. Wilson and C. L. Hussey, *Inorg. Chem.*, 1982, **21**, 1263.
30 A. K. Abdul-Sala, A. M. Greenway, K. R. Seddon and T. Welton, *Org. Mass Spectrom.*, 1993, **28**, 759; A. K. Abdul-Sala, A. E. Elaiwi, A. M. Greenway and K. R. Seddon, *Eur. Mass Spectrom.*, 1997, **3**, 245.
31 J. Fuller, R. T. Carlin, H. C. De Long and D. Haworth, *J. Chem. Soc., Chem. Commun.*, 1994, 299.
32 See, *e.g.*: A. K. Abdul-Sala, A. M. Greenway, P. B. Hitchcock, T. J. Mohammed, K. R. Seddon and J. A. Zora, *J. Chem. Soc., Chem. Commun.*, 1986, 1753; P. B. Hitchcock, R. J. Lewis and T. Welton, *Polyhedron*, 1993, **12**, 2039; P. B. Hitchcock, K. R. Seddon and T. Welton, *J. Chem. Soc., Dalton Trans,* 1995, 3467.
33 M. R. Ciajolo, P. Corradini and V. Pavone, *Acta Crystallogr., Sect. B*, 1977, **33**, 553.
34 H. H. Paradies and F. Habben, *Acta Crystallogr.*, *Sect. C*, 1993, **49**, 744.
35 P. B. Hitchcock, K. R. Seddon and T. Welton, *J. Chem. Soc., Dalton Trans.*, 1993, 2639.
36 H. Sackmann and D. Demus, *Mol. Cryst. Liq. Cryst.*, 1973, **21**, 239.
37 M. Tabrizian, A. Soldera, M. Couturier and C. G. Bazuin, *Liq. Cryst.*, 1995, **18**, 475.
38 H. L. Casal, D. G. Cameron and H. H. Mantsch, *J. Phys. Chem.*, 1985, **89**, 5557.

Paper 8/06169F